International Journal of Physical Sciences Vol. 5(3), pp. 226-237, March 2010
Available online at http://www.academicjournals.org/IJPS
ISSN 1992 - 1950 © 2010 Academic Journals

Full Length Research Paper

The comparison of analytical and numerical solutions for wave diffraction due to insular breakwater

Sung-Duk Kim[1] and Ho Jin Lee[2]*

[1]Chung-Ang University, Department of Civil and Environmental Engineering, 221, Seoul, Korea.
[2]Colorado State University, Department of Civil and Environmental Engineering, Fort Collins, CO 80523, USA.

Accepted 15 February, 2010

This study has investigated the wave diffraction due to insular breakwater using analytical solutions based on the Fresnel integral and Polynomial approximation solution of Fresnel integrals, and numerical solutions of boundary element method (BEM) based on the boundary integral equation. When using the Fresnel integrals the mathematical equations and the boundary conditions became complicated, but when using the Polynomial approximation solution these things became less complex and were able to be expressed in more simple terms. Using the Polynomial approximation solution also allowed for a fast approach to going through a great deal of data. The BEM allowed for the simplification of input data, the reduction of memory usage and the allowance of measuring the physical quantity within the boundary. The results of wave diffraction derived from the three methods were compared through implementation of various calculation conditions and has been expressed through graphs and contours. This study aims to provide information on how to use the polynomial approximation solution and the BEM instead of the Fresnel integrals in many practical situations and also in regions or wave fields where a great amount of calculation time is required in order to figure out wave diffraction problems.

Key words: Wave diffraction, insular breakwater, Fresnel integral, polynomial approximation solution, boundary element method.

INTRODUCTION

When constructing breakwaters in order to obtain stillness in harbors and fishery port, the investigation of the diffraction problem due to the breakwater still receives a large interest in the field of coastal and ocean engineering. With the basis of Sommerfeld's (1886) wave diffraction theory, Penny and Price (1944, 1952) have presented the wave diffraction theory due to infinite breakwater. By the research of Blue and Johnson (1949), Johnson (1952), Weigel et al. (1962) and, Wiegel (1964), the wave diffraction due to gap type breakwater has been used widely in the field of coastal engineering. Also hailed as a method to consider the mild slope of water depth, the research of Pos and Kilner (1987) has used the mild slope equation based on the finite element method (FEM) to conduct numerical calculations. Hunt (1990) has used the first kind of Fredholm integral equation to calculate the wave interval passing through the gap of the gap type breakwater. Dalrymple and Martin (1990) used the eigenvalue - expansion approach to study the diffraction problem due to in - line segments of break-waters. Abul-Azm and Willimas (1997) also used the eigenvalue - expansion approach to study the diffraction problem due to non-collinear segment of breakwaters. Wiliams and Crull (1993), and Wiliams et al. (1995) applied the boundary integral equation based on the Green function on diffraction problems. Also, Briggs et al. (1995) used a physical model in the wave basin to experiment with the diffraction caused by infinite breakwaters. Besides these, the solution to wave diffraction can be solved through the Fourier series and the eigenvalue-expansion approach, but these approaches take a long time calculating, and in complex harbors it is difficult to set boundary conditions.

In order to overcome these obstacles this study has reviewed the polynomial approximations and has studied the diffraction problems of insular breakwaters. The Fresnel integrals that were an analytical solution that has been traditionally used were reviewed under the same

*Corresponding author. E-mail:leehojin74@gmail.com.

conditions as the former method, and the theories of both sides were compared. The efficiency of numerical calculation time of diffraction and the accuracy of both theories were investigated. Also the numerical analysis of the BEM was applied to insular breakwater and compared to the two analytical solutions. The results obtained herein by this study provide information on how the results of BEM approach the results of both analytical solutions such as the Fresnel integral and the polynomial approximation for the wave diffraction by insular breakwater. Excellent agreement exists for both analytical solutions. Regarding the diffraction wave height, in small areas the numerical results have a slightly lower height than those of the analytical results, however apart from these areas there has been good agreement between the BEM and the analytical solutions.

To perform analytical and numerical calculations, first, insular breakwater needs to be displayed as an upright wall that is in a straight line. The length of the insular breakwater is designated as 1.0 and 4.0 *L* (*L* = wavelength), the wave period is ranged at 10 seconds and the incident wave angle is 90° and 60°. The present study was investigated for four cases of conditions of calculations.

THEORETICAL DEVELOPMENT

Analytical solutions for wave diffraction due to insular breakwater

The geometry of the problem is presented in Figure 1. In order to solve the problem of diffraction in insular breakwaters the theoretical calculation is performed. As shown in Figure 1, the left wave field of the breakwater is indicated as 1 and the right wave field is indicated as 2. Assuming that the fluid is inviscid, incompressible, and the flow irrotational, then the fluid motion in each of the fluid regions may be described in terms of velocity potentials $\Phi = \psi(x,y)\cosh k(h+z)e^{ik\omega t}$ and wave elevation $\varsigma = \psi(x,y)e^{ik\omega t}$. The velocity potential satisfy the Laplace equation, and then the Helmholtz equation may be written as;

$$\frac{\partial^2\psi(x,y)}{\partial x^2}+\frac{\partial^2\psi(x,y)}{\partial y^2}+k\psi(x,y)=0 \quad (1)$$

Equation (1) can be expressed by polar coordinate (*r*, *θ*) as Equation (2)

$$\frac{\partial^2\psi(r,\theta)}{\partial r^2}+\frac{1}{r}\frac{\partial^2\psi(r,\theta)}{\partial r^2}+\frac{1}{r^2}\frac{\partial^2\psi(r,\theta)}{\partial\theta^2}+k\psi(r,\theta)=0 \quad (2)$$

The boundary conditions on the free-surface and sea-bed can be expressed in the following form,

$$\frac{\partial\psi}{\partial z}-\frac{\omega^2\psi}{g}=0 \text{ on } z=0 \quad (3)$$

$$\frac{\partial\psi}{\partial z}=0 \text{ on } z=-h \quad (4)$$

Where; *g* is the acceleration due to gravity. The flow perpendicular to the side of the wall is zero at the boundary surface adjoined to breakwater. Taking equation (2) by two kinds of conditions, the solution of diffraction by insular breakwater can be can be written,

$$\psi_i(r_i,\theta_i)=f(u_{ij})e^{-i\{kr_i\cos(\theta_i-\Theta_i)-2\pi\varepsilon\}}+g(\sigma_{ij})e^{-i\{kr_i\cos(\theta_i+\Theta_i)-2\pi\varepsilon\}}$$

(*i* and *j*=1,2) (5)

Where; ε is to modify the phase difference of the incident wave between the two wave fields of the breakwater, *k* is the wave number, and

$$u_{ij}=2\sqrt{kr_i/\pi}\sin\frac{\theta_i-\Theta_i}{2} \quad (i \text{ and } j=1,2)$$

$$\sigma_{ij}=-2\sqrt{kr_i/\pi}\sin\frac{\theta_i+\Theta_i}{2} \quad (i \text{ and } j=1,2)$$

$$f(u_{ij})=\frac{1}{\sqrt{2}}e^{i\pi/4}\int_{\infty}^{u_{ij}}e^{-i\pi\omega^2/2}d\omega \quad (i \text{ and } j=1,2)$$

$$g(\sigma_{ij})=\frac{1}{\sqrt{2}}e^{i\pi/4}\int_{\infty}^{\sigma_{ij}}e^{-i\pi\omega^2/2}d\omega \quad (i \text{ and } j=1,2) \quad (6)$$

When; u_{ij} and σ_{ij} are positive, which means the incident region is

$$f(u_{ij})=\frac{1}{\sqrt{2}}e^{i\pi/4}\int_{\infty}^{u_{ij}}e^{-i\pi\omega^2/2}d\omega=\frac{1}{\sqrt{2}}e^{i\pi/4}\left[\int_{0}^{\infty}e^{-i\pi\omega^2/2}d\omega+\frac{1}{\sqrt{2}}e^{i\pi/4}\int_{0}^{u_{ij}}e^{-i\pi\omega^2/2}d\omega\right]$$

$$=\frac{1}{\sqrt{2}}e^{i\pi/4}\left[\frac{1}{2}(1-i)+\{C(u_{ij})-iS(u_{ij})\}\right]=\frac{1}{2}\left[\{1+C(u_{ij})+S(u_{ij})\}+i\{C(u_{ij})-S(u_{ij})\}\right]$$

(*i* and *j*=1,2) (7)

$$g(\sigma_{ij})=\frac{1}{\sqrt{2}}e^{i\pi/4}\int_{\infty}^{\sigma_{ij}}e^{-i\pi\omega^2/2}d\omega=\frac{1}{\sqrt{2}}e^{i\pi/4}\left[\int_{0}^{\infty}e^{-i\pi\omega^2/2}d\omega+\frac{1}{\sqrt{2}}e^{i\pi/4}\int_{0}^{\sigma_{ij}}e^{-i\pi\omega^2/2}d\omega\right]$$

$$=\frac{1}{\sqrt{2}}e^{i\pi/4}\left[\frac{1}{2}(1-i)+\{C(\sigma_{ij})-iS(\sigma_{ij})\}\right]=\frac{1}{2}\left[\{1+C(\sigma_{ij})+S(\sigma_{ij})\}+i\{C(\sigma_{ij})-S(\sigma_{ij})\}\right]$$

(*i* and *j*=1,2) (8)

When u_{ij} and σ_{ij} are negative, which means the diffracted region is;

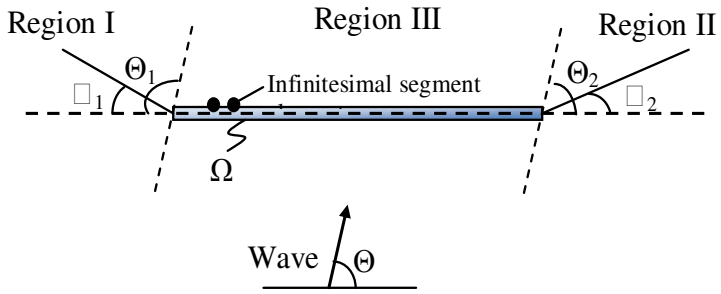

Figure 1. Definition sketch of the inclined incident wave propagated to the insular breakwater.

$$f(-u_{ij})=\frac{1}{\sqrt{2}}e^{i\pi/4}\int_{-\infty}^{t_{ij}}e^{-i\pi\omega^2/2}d\omega=\frac{1}{\sqrt{2}}e^{i\pi/4}\int_{t_{ij}}^{\infty}e^{-i\pi\omega^2/2}d\omega=\frac{1}{\sqrt{2}}e^{i\pi/4}\left[\int_{0}^{\infty}e^{-i\pi\omega^2/2}d\omega-\frac{1}{\sqrt{2}}e^{i\pi/4}\int_{0}^{t_{ij}}e^{-i\pi\omega^2/2}d\omega\right]$$

$$=\frac{1}{\sqrt{2}}e^{i\pi/4}\left[\frac{1}{2}(1-i)-\{C(u_{ij})-iS(u_{ij})\}\right]=\frac{1}{2}\left[\{1-C(u_{ij})-S(u_{ij})\}+i\{S(u_{ij})-C(u_{ij})\}\right]$$

(*i* and *j*=1,2) (9)

$$g(-\sigma_{ij})=\frac{1}{\sqrt{2}}e^{i\pi/4}\int_{-\infty}^{\sigma_{ij}}e^{-i\pi\omega^2/2}d\omega=\frac{1}{\sqrt{2}}e^{i\pi/4}\int_{\sigma_{ij}}^{\infty}e^{-i\pi\omega^2/2}d\omega=\frac{1}{\sqrt{2}}e^{i\pi/4}\left[\int_{0}^{\infty}e^{-i\pi\omega^2/2}d\omega-\frac{1}{\sqrt{2}}e^{i\pi/4}\int_{0}^{\sigma_{ij}}e^{-i\pi\omega^2/2}d\omega\right]$$

$$=\frac{1}{\sqrt{2}}e^{i\pi/4}\left[\frac{1}{2}(1-i)-\{C(\sigma_{ij})-iS(\sigma_{ij})\}\right]=\frac{1}{2}\left[\{1-C(\sigma_{ij})-S(\sigma_{ij})\}+i\{S(\sigma_{ij})-C(\sigma_{ij})\}\right]$$

(*I* and*j*=1,2) (10)

Where; $C(\lambda_{ij})$, $S(\lambda_{ij})$ are Fresnel integrals, at this time λ_{ij} is u_{ij} or σ_{ij}, and can be defined as equation (11)

$$C(\lambda_{ij})=\int_0^{\lambda_{ij}}\cos\frac{\pi}{2}\omega^2 d\omega\ ,\ S(\lambda_{ij})=\int_0^{\lambda_{ij}}\sin\frac{\pi}{2}\omega^2 d\omega \tag{11}$$

We can replace the Fresnel integrals by the polynomial approximations in the above equations. The diffraction analysis can be simplified by using the polynomial approximations of the Fresnel integrals.

$$C(\lambda_{ij})=-C(-\lambda_{ij})\cong 0.5+\frac{(1+0.926\lambda_{ij})\sin(\frac{\pi}{2}\lambda_{ij}^2)}{2+1.792\lambda_{ij}+3.104\lambda_{ij}^2}-\frac{\cos(\frac{\pi}{2}\lambda_{ij}^2)}{2+4.142\lambda_{ij}+3.492\lambda_{ij}^2+6.670\lambda_{ij}^3}+\delta(\lambda_{ij}) \tag{12}$$

or value of λ_{ij}, that is where $0\le\lambda_{ij}\le\infty$, and

$$S(\lambda_{ij})=-S(-\lambda_{ij})\cong 0.5-\frac{(1+0.926\lambda_{ij})\cos(\frac{\pi}{2}\lambda_{ij}^2)}{2+1.792\lambda_{ij}+3.104\lambda_{ij}^2}-\frac{\sin(\frac{\pi}{2}\lambda_{ij}^2)}{2+4.142\lambda_{ij}+3.492\lambda_{ij}^2+6.670\lambda_{ij}^3}+\delta(\lambda_{ij}) \tag{13}$$

Where the remainder for both equations is $\delta(\lambda_{ij})\le 0.002$.

If the real and imagined parts of function $f(u_{ij})$ and $g(\sigma_{ij})$ may be expressed as V_{ij} and W_{ij} respectively, the following can be written as;

$$f(-u_{ij})=V_{ij}+iW_{ij}\ ,\ g(-\sigma_{ij})=V_{ij}+iW_{ij}\ \ (i \text{ and } j=1,2) \tag{14}$$

$$V_{ij}=\frac{1}{2}\{1-(C(\lambda_{ij})-S(\lambda_{ij})\}\ ,\ W_{ij}=\frac{1}{2}\{S(\lambda_{ij})-C(\lambda_{ij})\}\ \ (I \text{ and } j=1,2) \tag{15}$$

Diffraction coefficient of K_{dij} can be written as;

$$K_{dij}=\sqrt{\psi_i(r_i,\theta_i)^2} \tag{16}$$

Numerical solutions for wave diffraction due to insular breakwater

The boundary region is expressed as Ω (insular breakwater boundary), and the length of the breakwater is expressed as *B*. The offshore structure is subject to a train of regular component waves of angular frequency ω propagating at angle Θ to the positive *x*-axis. The wave diffraction due to insular breakwater using the boundary element method based on the Green's second identity is obtained, and boundary of breakwater is divided by infinitesimal segment in Figure 1. The wave function $\psi(x,y)$ in equation (1) can be written as:

$$\psi(x,y)=\psi_I(x,y)+\psi_R(x,y)+\psi_S(x,y) \tag{17}$$

Where; $\psi_I(x,y)$, $\psi_R(x,y)$, and $\psi_s(x,y)$ are incident, reflected, and scattered wave function, respectively. $\psi_I(x,y)$ and $\psi_R(x,y)$ can be expressed as:

$$\left.\begin{aligned}\psi_I(x,y)&=-ie^{-ik(x\cos\Theta+y\sin\Theta)}\\ \psi_R(x,y)&=-ie^{-ik(x\cos\Theta-y\sin\Theta)}\end{aligned}\right\} \tag{18}$$

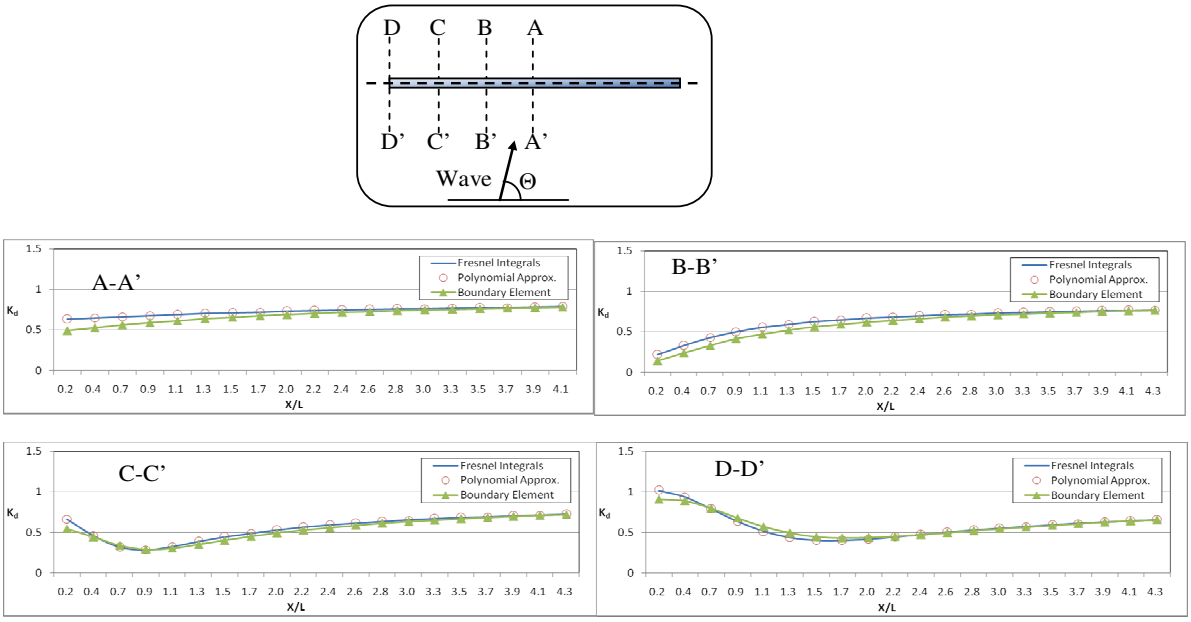

Figure 2. Comparisons of diffraction coefficients at the vicinity of the breakwater for the length of breakwater B =1.0L and incident wave angle.

Applying Green's second identity to $\psi_S(x,y)$ over the fluid domain, the following integral equation can be expressed as:

$$\psi_S(x,y) = -\frac{i}{4}\int_{\Omega}\left\{\psi_S(\xi,\eta)\frac{\partial}{\partial n}(H_0^{(1)}(kR)) - \frac{\partial\psi_S(\xi,\eta)}{\partial n}(H_0^{(1)}(kR))\right\}d\Omega \quad (19)$$

Where; $H_0^{(1)}$ is the Hankel function of the first kind of order zero, (x,y) is the point of the fluid region, (ξ,η) is the boundary point of breakwater, and $R=\sqrt{(x-\xi)^2+(y-\eta)^2}$.

The diffraction coefficient at the point of the fluid region (x,y) can yield,

$$K_d = \left|\psi_I(x,y) + \psi_S(x,y)\right| \quad (20)$$

RESULTS AND DISCUSSION

The numerical computational program has been developed to implement the above theories, which are the Fresnel integrals, the polynomial approximation of Fresnel integrals, and the boundary element method (BEM) using the Green function, for the regular wave diffraction due to insular breakwater. Numerical and analytical examples are presented to investigate the comparisons of three solutions (Fresnel integrals, polynomial approxi-mations, and BEM) for the diffraction due to insular breakwater with different length of breakwater and different incident wave angles. In this study, the condition of calculations are water depth at the vicinity of fluid region h = 10 m, wave period t = 10 s, incident wave angle $\Theta = 90^\circ$ and 60°, and the length of breakwater B=1.0L and B = 4.0 L, respectively. Figure 2 presents the results for the diffraction coefficient obtained by the analytical solutions and numerical solutions, where the spatial variations of the diffraction coefficient are illustrated along the four selected sections, A-A', B-B', C-C', and D-D' in the case of B = 1.0 L and $\Theta = 90^\circ$. In all cases, excellent agreement has been made between the Fresnel integrals and the polynomial approximations. When comparing the numerical solutions (BEM) to the analytical solutions, good agreement has been shown between the two solutions but at the center line (A-A') and B-B' line, diffraction coefficients by numerical solutions show to be slightly lower than the diffraction coefficients by analytical solutions. The reason behind this discrepancy is that in analytical solutions the boundaries are set in a straight line while in BEM the boundaries are divided into infinitesimal segments. As the diffraction coefficient moves away from the boundary elements (the part that is right behind the breakwater = x/L = 0.2~1.5) the two solutions fall into better agreement.

Figure 3 presents the results for the diffraction coefficient obtained by the analytical solutions and numerical solutions, where the spatial variations of the diffraction coefficient are illustrated along 7 selected sections, A-A', B-B', C-C', D-D', E-E', F-F', and G-G' in the case of B = 1.0 L and $\Theta = 60^\circ$. In all cases, excellent agreement has been made between the Fresnel integrals and the polynomial

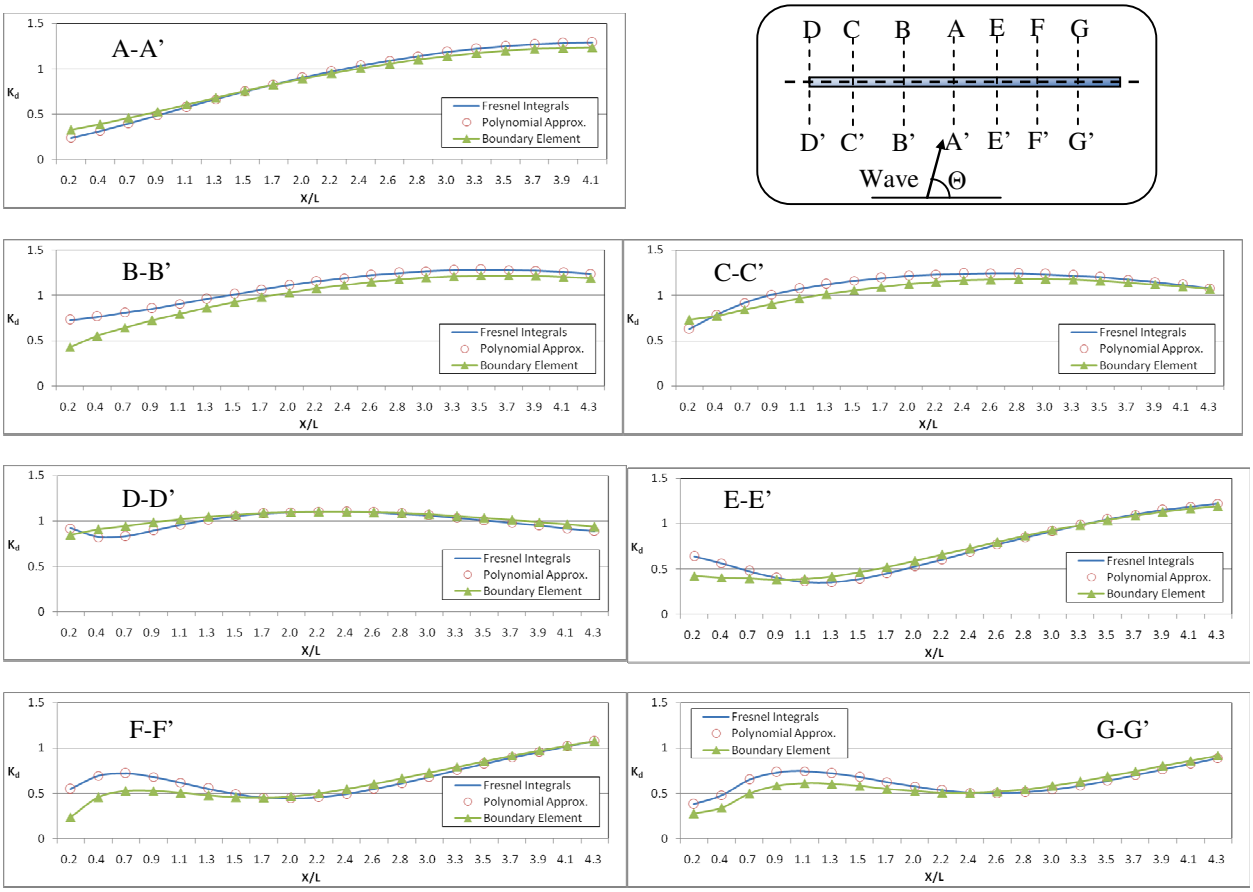

Figure 3. Comparisons of diffraction coefficients at the vicinity of the breakwater for the length of breakwater B=1.0L and incident wave angle $\Theta = 60^{\circ}$.

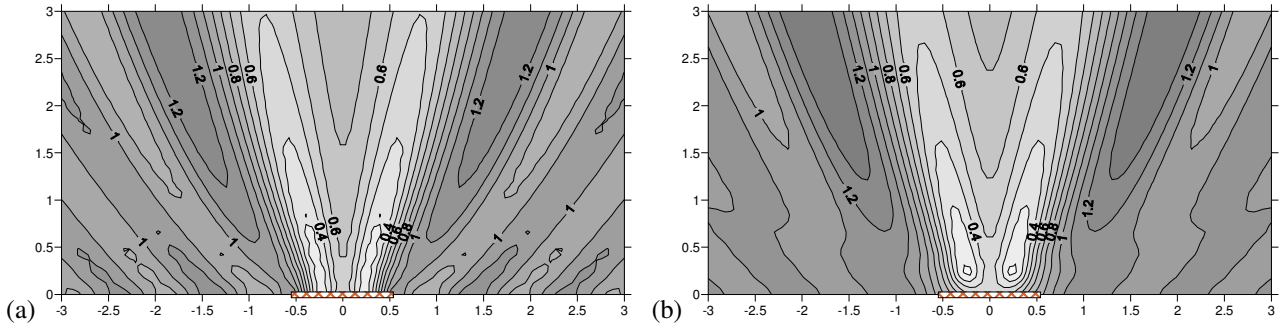

Figure 4. The wave diffraction contour plots for the length of breakwater B=1.0L and incident wave angle $\Theta = 90^{\circ}$ (a) analytical solutions, (b) numerical solutions.

approximations. When comparing the numerical solutions (BEM) to the analytical solutions show good agreement, but at the B-B' line and the C-C' line (left side of breakwater) the diffraction coefficients by numerical solutions have slightly lower diffraction coefficients than those of the analytical solutions. This is due to the fewer wave mode numbers that were scattered by wave oblique wave propagation on insular breakwater in the case of BEM. From these analyses, we notice that the overall wave height distributions of the wave field may be found in the vicinity of the insular breakwater with a contour plot. Figure 4 presents the contours of the wave height ratios

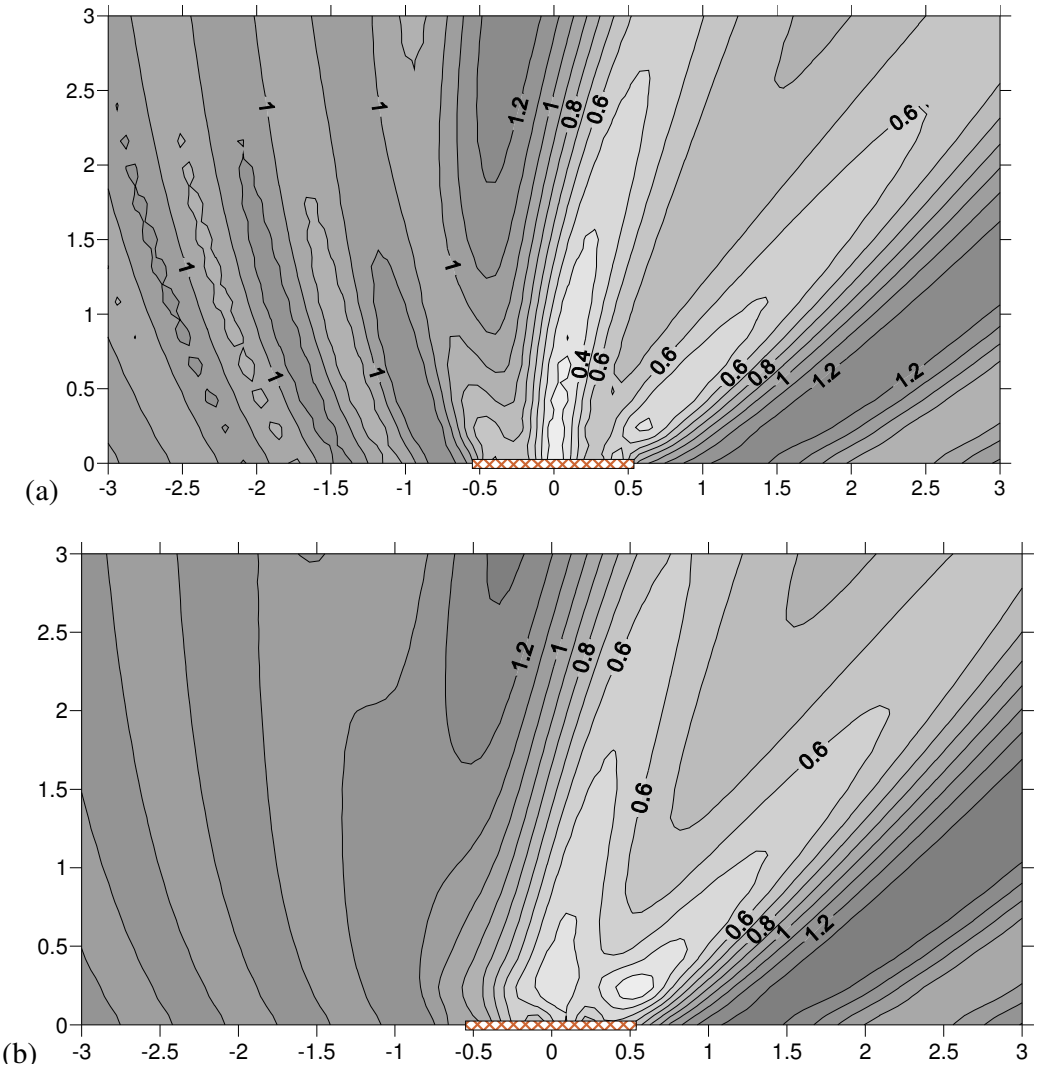

Figure 5. The wave diffraction contour plots for the length of breakwater B=1.0L and incident wave angle $\Theta = 60^{\circ}$ (a) analytical solutions, (b) numerical solutions.

due to wave diffraction by insular breakwater for the two cases described above in the case of B = 1.0L and $\Theta = 90^{\circ}$. Overall the contour plot of the two solutions showed a similar pattern. However the analytical solutions in Figure 4 (a) have more scattering and incident wave mode numbers than the numerical solutions in Figure 4 (b). This is because the numerical solutions have been approximated and thus the number of wave modes is shown to be fewer and the wave band has appeared as being wide. Figure 5 presents the contours of the wave height ratios due to wave diffraction by insular breakwater for the two cases described above in the case of B =1.0L and $\Theta = 60^{\circ}$. It has a similar tendency as in the case of the normal incidence of wave angle, but at the left wave field of the breakwater, namely the incident wave region, the wave height distributions are smoothing due to numerical approximation. Figures 6 and 7 present three dimensional projection contours of the wave height ratios due to wave diffraction by insular breakwater for the two cases described above in the case of B = 1.0L.

Figure 8 presents the results for the diffraction coefficient obtained by the analytical solutions and the numerical solutions, where the spatial variations of the diffraction coefficient are illustrated along the four selected sections, A-A', B-B', C-C', and D-D' in the case of B=4.0L and $\Theta = 90^{\circ}$. In all cases, excellent agreement has been made between the Fresnel integrals and the polynomial approximations. When comparing the numerical solutions (BEM) to the analytical solutions, good agreement has been shown between the two solutions, but at the center line (A-A') the diffraction coefficients by numerical solutions show to be slightly lower than the diffraction coefficients by analytical solutions in a

(a)

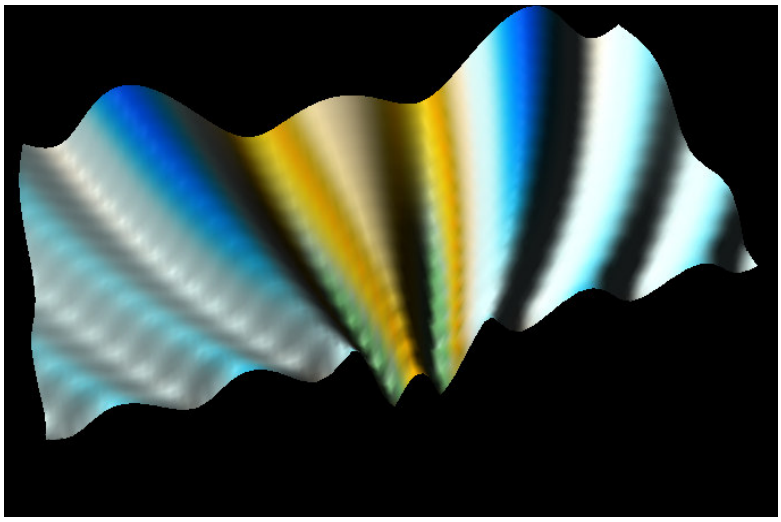

(b)

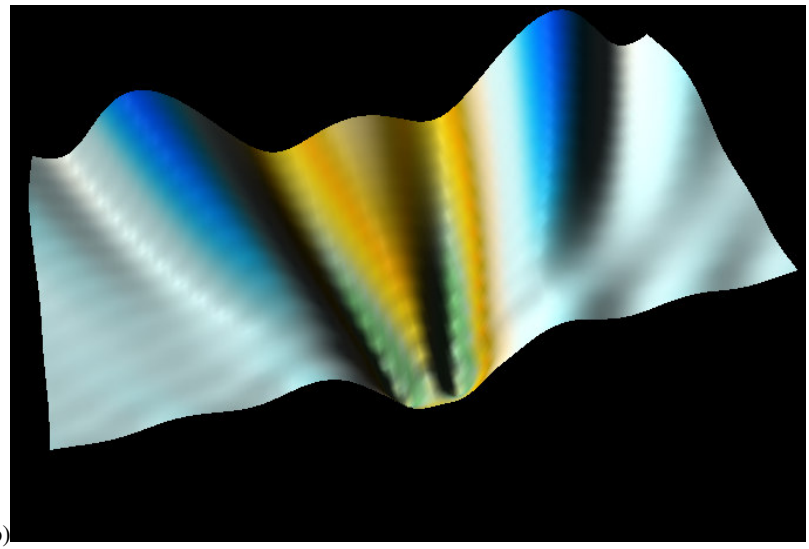

Figure 6. The wave diffraction (3D) for the length of breakwater B=1.0L and incident wave angle $\Theta = 90^{\circ}$ (a) analytical solutions, (b) numerical solutions.

(a)

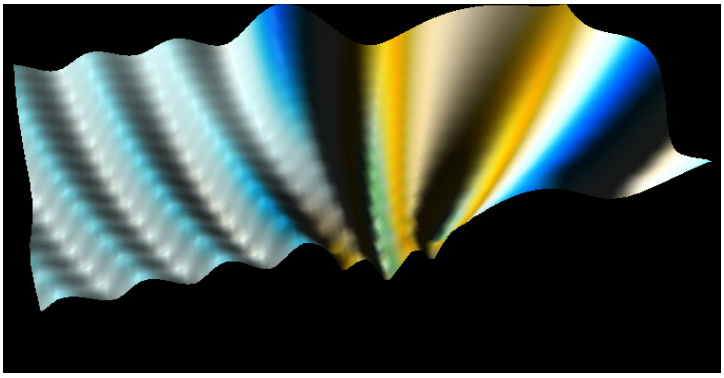

(b)

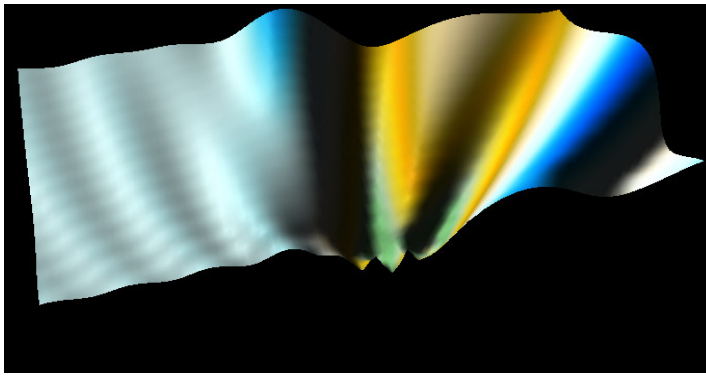

Figure 7. The wave diffraction (3D) for the length of breakwater B=1.0L and incident wave angle $\Theta = 60^{\circ}$ (a) analytical solutions, (b) numerical solutions.

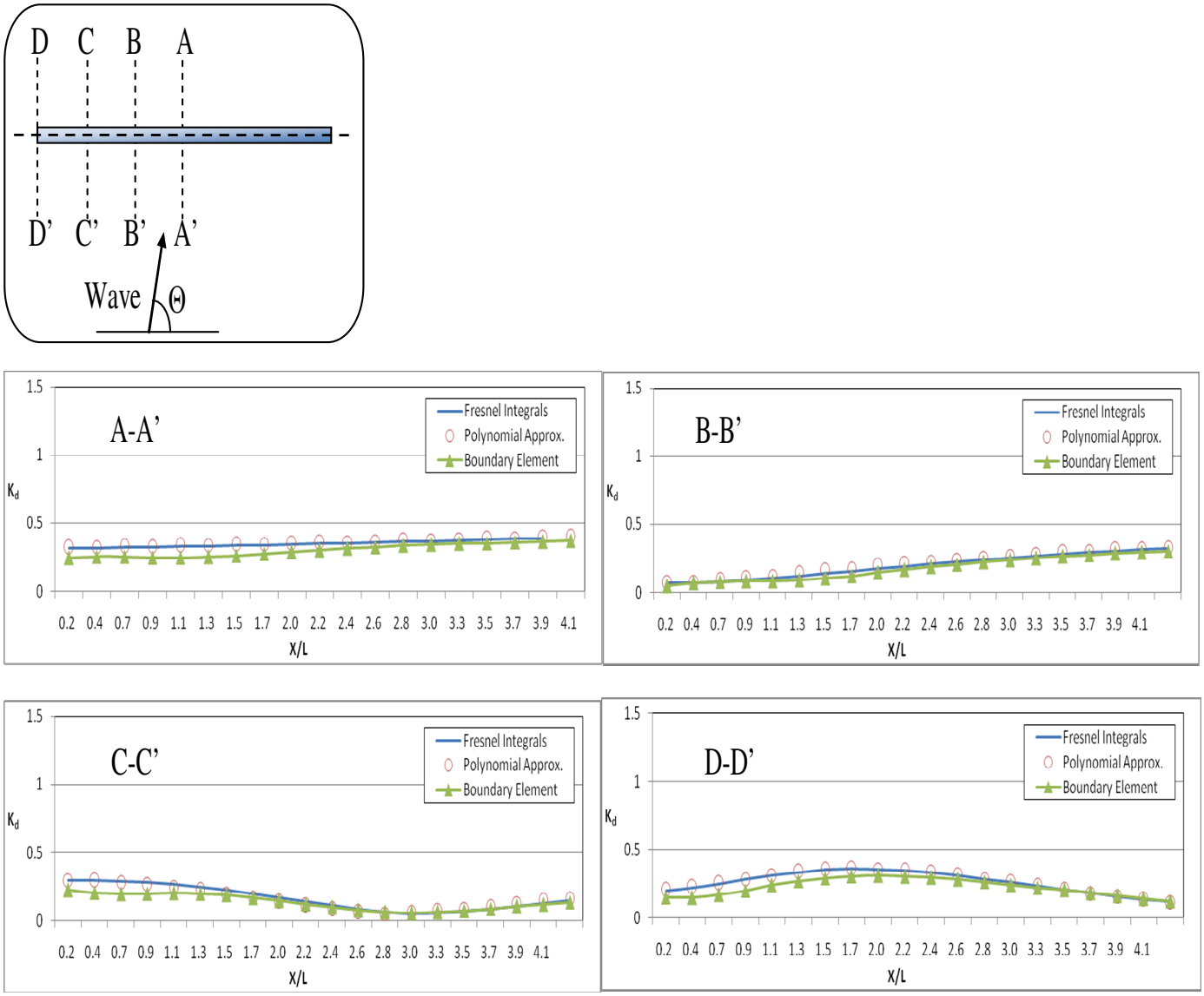

Figure 8. Comparisons of diffraction coefficients at the vicinity of the breakwater for the length of breakwater B=4.0L and incident wave angle $\Theta = 90^{\circ}$.

long range. This is because the breakwater has become longer and the boundary element has subsequently increased.

Figure 9 presents the results for the diffraction coefficient obtained by the analytical solutions and numerical solutions, where the spatial variations of the diffraction coefficient are illustrated along 7 selected sections, A-A', B-B', C-C', D-D', E-E', F-F', and G-G' in the case of B = 4.0L and $\Theta = 60^{\circ}$. When comparing the numerical solutions (BEM) to the analytical solutions, good agreement has been shown between the two solutions, but at the center lines (A-A') the diffraction coefficients by numerical solutions have slightly lower diffraction coefficients than those of the analytical solutions. This is because the center line is close to the boundary of the breakwater.

Figure 10 presents the contours of the wave height ratios due to wave diffraction by insular breakwater for the two cases described above in the case of B = 4.0L and $\Theta = 90^{\circ}$. Overall the contour plot of the two solutions showed a similar pattern, and these patterns fell in higher alignment at 4.0L than at 1.0L. At 4.0L the wave bandwidth was narrower than at 1.0L. Figure 11 presents the contours of the wave height ratios due to wave diffraction by insular breakwater for the two cases described above in the case of B = 4.0L and $\Theta = 60^{\circ}$. The numerical solutions have been approximated, therefore the number of wave modes has appeared as fewer, and the wave bandwidth is wider. Figure 12 and 13 present three dimensional projection contours of the wave height ratios due to wave diffraction by insular breakwater for

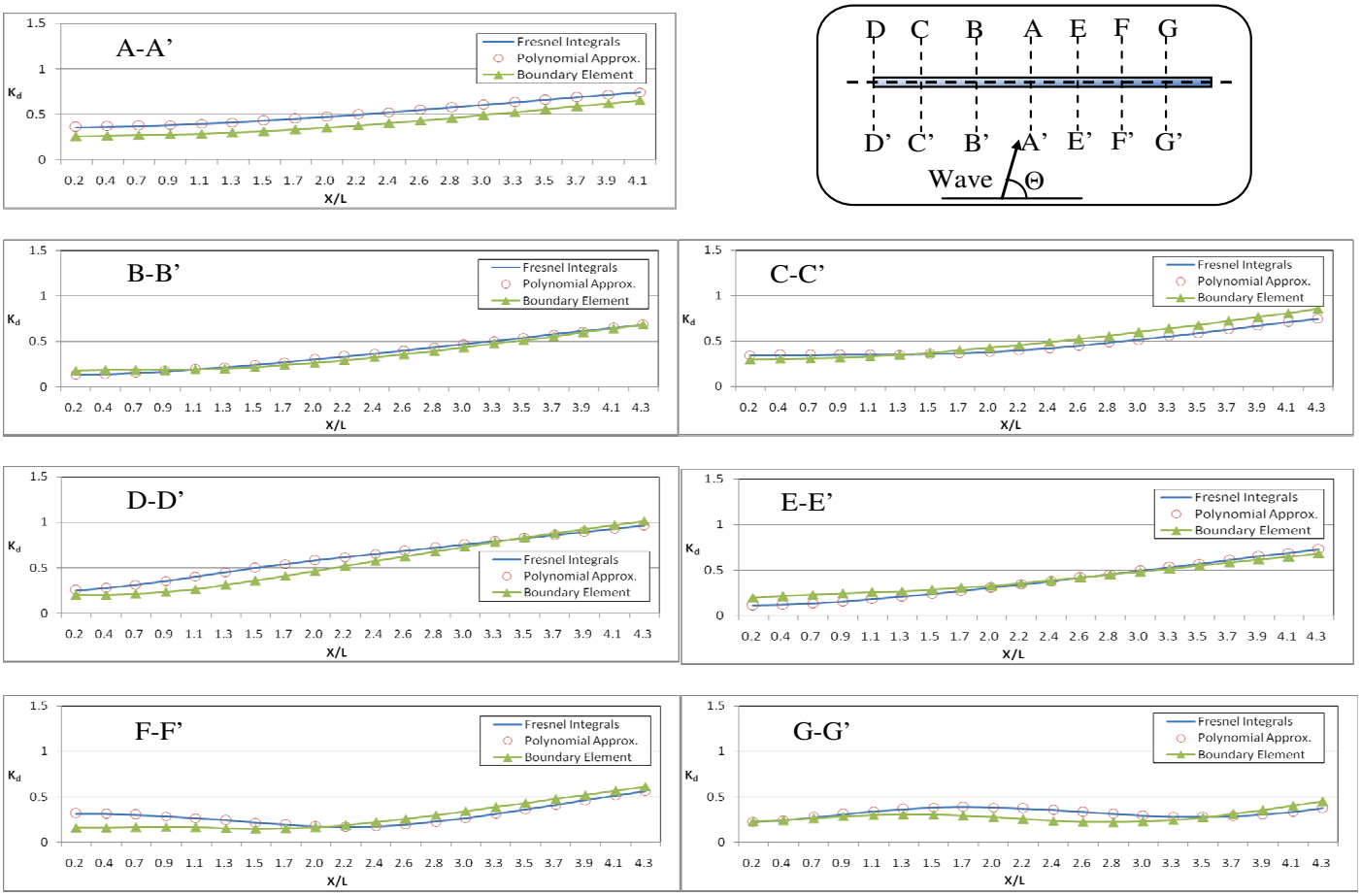

Figure 9. Comparisons of diffraction coefficients at the vicinity of the breakwater for the length of breakwater B=4.0L and incident wave angle $\Theta = 60^{\circ}$.

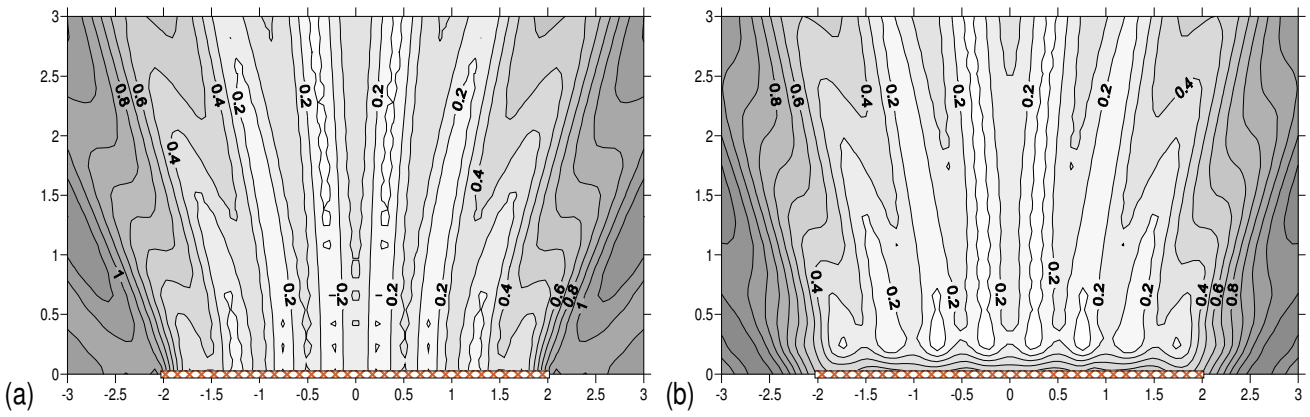

Figure 10. The wave diffraction contour plots for the length of breakwater B=4.0L and incident wave angle $\Theta = 90^{\circ}$ (a) analytical solutions, (b) numerical solutions.

the two cases described above in the case of B = 4.0 L. The results of the analytical solutions and the results of the numerical solutions were compared using the root mean square (RMS) method. This method was used by Walsh (1992) and Briggs et al. (1995) and the equation is as follows,

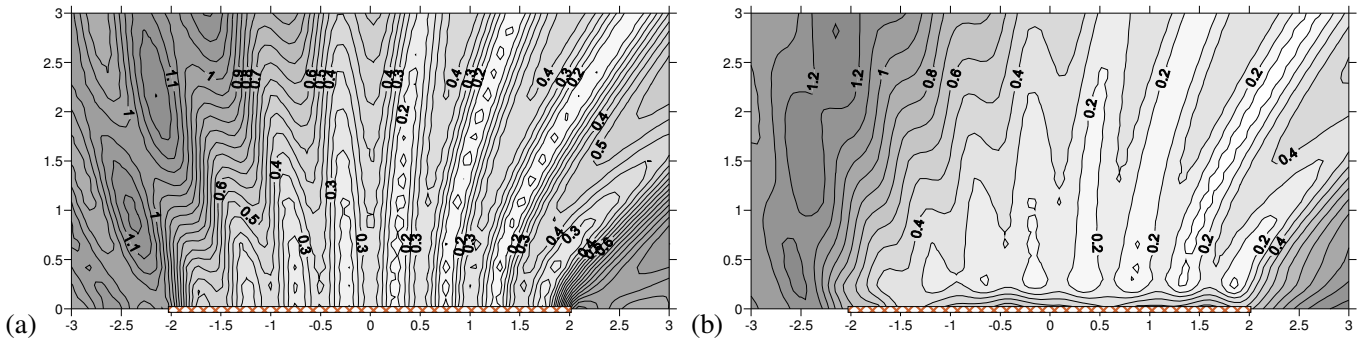

Figure 11. The wave diffraction contour plots for the length of breakwater B = 4.0 L and incident wave angle $\Theta = 60^{\circ}$ (a) analytical solutions, (b) numerical solutions.

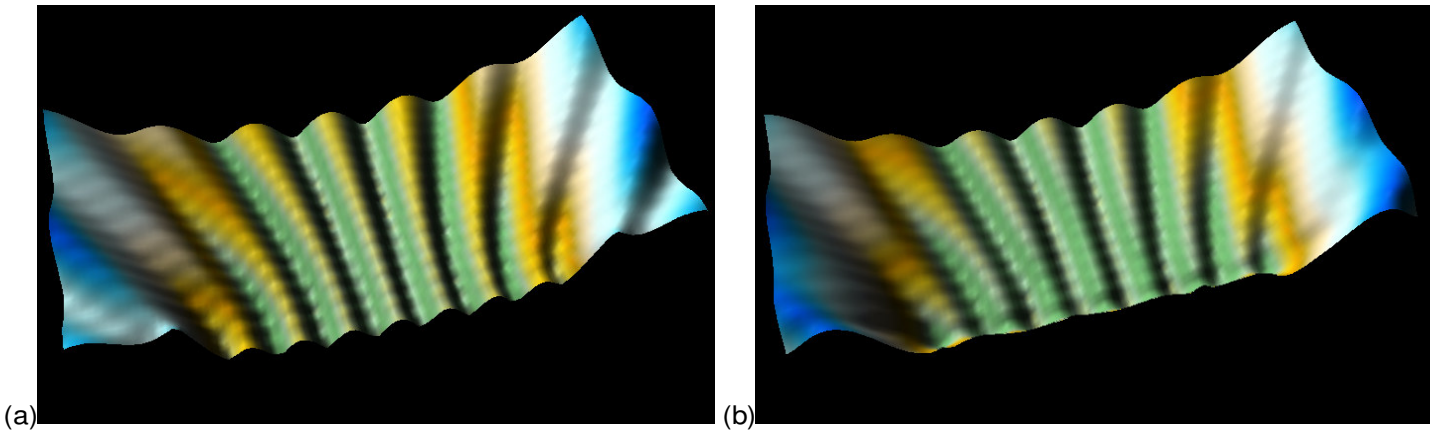

Figure 12. The wave diffraction (3D) for the length of breakwater B = 4.0 L and incident wave angle $\Theta = 90^{\circ}$ (a) analytical solutions, (b) numerical solutions.

$$RMS_{K_d} = \sqrt{\frac{\sum_{i=1}^{NP}\left\{(K_d)_{Fresnel} - (K_d)_{BEM}\right\}^2}{NP}} \quad (21)$$

$$RMS_{K_d} = \sqrt{\frac{\sum_{i=1}^{NP}\left\{(K_d)_{Fresnel} - (K_d)_{P}\right\}^2}{NP}} \quad (22)$$

Where; $(K_d)_{Fresnel}$ is the diffraction coefficient by Fresnel integrals, $(K_d)_{BEM}$ is the diffraction coefficient by boundary element method (BEM), $(K_d)_P$ is the diffraction coefficient by polynomial approximations and NP is the number of points investigated. The results are listed in Table 1. In the case of comparing the Polynomial approximations to the Fresnel integrals, there was a difference that ranged from 0.09% to 0.2%, and this denotes an excellent agreement. In the case of the Numerical solution (BEM) there was a difference that ranged from 5 - 11% and this expresses relative agreement. The CPU time of a computer that is used in numerical analysis is a very important element in the engineering field. There needs to be a lot of data researched in a large area and the ability to cope with the different environments of various situations. As shown in Table 2, this study has compared the computer processing time of the analytical solutions and the numerical solution. Using the polynomial approximations reduced the calculating time by a great amount from using the Fresnel integrals. In the case of the BEM time was reduced by approximately 45%. This shows that using either the polynomial approximations or the BEM allows for a vast reduction in the computer CPU time and can reduce the pressure on a computer's CPU. With these benefits the

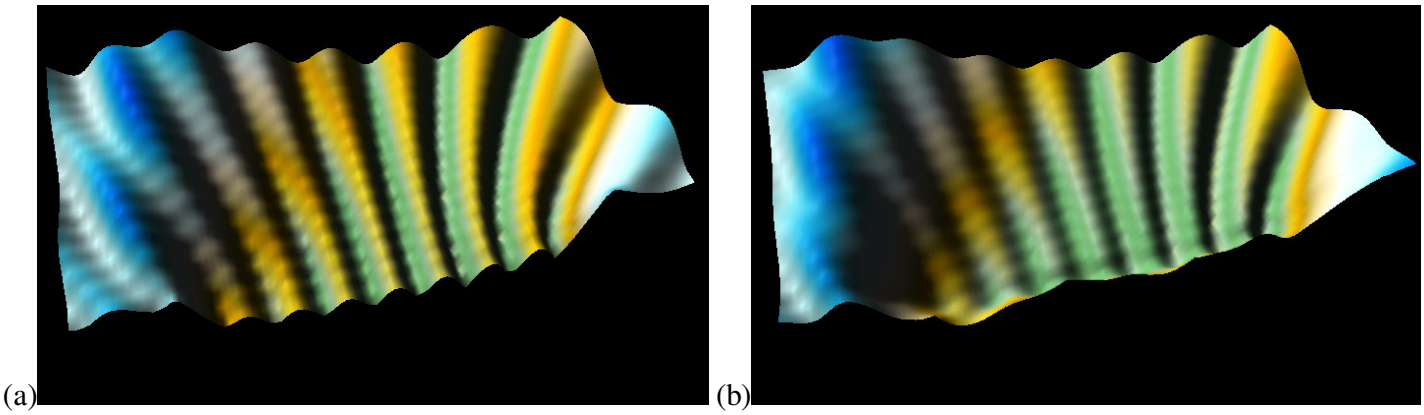

Figure 13. The wave diffraction (3D) for the length of breakwater B = 4.0 L and incident wave angle $\Theta = 90^{\circ}$ (a) analytical solutions, (b) numerical solutions.

Table 1. RMS differences between the results of the analytical solutions and the numerical solutions.

Incident wave angle	Length of breakwater			
	1.0 L		4.0 L	
	BEM	Polynomial	BEM	Polynomial
90°	0.07	0.0009	0.06	0.0028
60°	0.05	0.0012	0.11	0.0020

Table 2. Comparison of time taken to process data by each method.

Theory and time		Type of breakwater
		Insular breakwater with 1.0L (s)
Fresnel integrals	The elapsed time (seconds)	2.4
Polynomial approximations		0.28
Boundary Element Method		1.3

wave field, where insular breakwaters are set up, can be divided into many boundary regions and the data from these many regions can be calculated accurately, allowing for effective investigation of wider coastal fields.

Conclusion

The numerical computational program has been developed to implement the diffraction theory, Fresnel integrals, polynomial approximation, and boundary element method (BEM) using the Green function, for the regular wave diffraction due to insular breakwater. In all cases, excellent agreement was made between the Fresnel integrals and polynomial approximations. When comparing the numerical solutions (BEM) to the analytical solutions, there was relatively good agreement although there was a slight difference in the area right behind the breakwater. However this difference is due to the fact that the numerical solutions were approximated, whereby the number of wave modes appeared to be fewer and the wave bandwidth appeared wider. There was not a big difference in the RMS comparison among the three methods and this means that all three methods can be used in studying the diffraction of insular breakwaters. Also, by using the computer's internal routine the calculation time of each method was observed. The Polynomial approximation solutions reduced the calculation time to an extraordinary rate and the BEM was also able to reduce the calculation time by 45%. This will not only allow for a reduction in time in calculating a lot of data in different field research areas but it will also provide a means for accurate diffraction calculations. The information from this study can be applied to many different areas of coastal and ocean engineering and it is hoped that it will be used widely.

REFERENCES

Abul-Azm AG, Williams AN (1997). Oblique wave diffraction by segmented offshore breakwater. Ocean Eng. 24(1): 63-82.

Blue FL, Johnson JW (1949). Diffraction of sea waves passing through a breakwater gap. Trans. A.G.U. 30(5): 705-718.

Briggs MJ, Thompson EF, Vincent CL (1995). Wave diffraction around breakwater. J. Waterway, Port, Coastal, Ocean Eng., ASCE 121(1): 23-35.

Dalrymple RA, Martin PA (1990). Wave diffraction through offshore breakwaters. J. Waterway, Port, Coastal, Ocean Eng., ASCE 116(6): 727-741.

Hunt B (1990). An integral equation solution for the breakwater gap problem. J. Hydraulic Res. 28(5): 609-619.

Johnson JW (1952). Generalized wave diffraction diagrams. Proc. 2nd Conf. Coastal Engineering, Council on Wave Research, Eng. Found, 6-23.

Penny WG, Price AG (1952). The diffraction theory of sea waves and the shelter afforded by breakwater. Part I of some gravity wave problems in the motion of perfect liquids by Martin JC, Moyce WJ, Penny WG, Price AT and Thornhill CK. Philos. Trans. R. Soc. London, Ser. A 244: 236-253.

Penny WG, Price AG (1944). Diffraction of sea waves by breakwater. Artifical Harburs, Dire Misc. Weapon, Tech. His. 66: 56-78.

Pos JD, Kilner FA (1987). Breakwater gap wave diffraction: an experimental and numerical study. J. Waterway, Port, Coastal, and Ocean Eng. ASCE, 113(1): 1-21.

Sommerfeld A (1986). Mathematische theorie dier diffraction. Math. Annalen. 47: 317-374.

Walsh MT (1992). Diffraction of directional wave spectra around a semi-infinite breakwater. Misc. Paper CERC 92-5. U.S. Army Corps of Engineers (USACE). Waterway. Experiment Station, Vicksburg, Miss.

Weigel RL (1962). Diffraction of waves by semi-infinite breakwaters. J. of Hydraulic Div. Proceeding: ASCE 88(HY1): 27-44.

Williams AN, Crull TWW (1993). Wave diffraction by array of thin-screen breakwaters. J. Waterway, Port, Coastal, Ocean Eng. ASCE 119(6): 606-617.

Williams AN, Vasquez JH, Crull TWW (1995). Oblique-wave diffraction by noncollinear segmented offshore breakwater. J. Waterway, Port, Coastal, Ocean Eng. ASCE 121(6): 326-333.